Silicon oxide contact hole etching employing an environmentally benign process

Kazushi Fujita, Masaru Hori,[a] and Toshio Goto
Department of Quantum Engineering, School of Engineering, Nagoya University, Furo-cho, Chikusa-ku, Nagoya 464-8603, Japan

Masafumi Ito
Department of Opto-Mechatronics, Faculty of Systems Engineering, Wakayama University, 930 Sakaedani Wakayama 640-8510, Japan

(Received 29 January 2002; accepted 19 August 2002)

An environmentally benign etching process using a solid material evaporation technique has been investigated for preventing global warming. In this process, a polytetrafluoroethylene is evaporated by a CO_2 laser, resulting in production of fluorocarbon species working as the etching species. Therefore, this system employs no perfluorocompound feed gases, which cause global warming, and enables us to design a new plasma chemistry using the solid material. The system was successfully applied to a SiO_2 contact hole etching process employing a planar electron cyclotron resonance plasma. The etched profile was successfully controlled by varying the Ar dilution ratio and the process pressure. In a 0.6 μm contact hole and a 0.08 μm trench fabrication process, this novel process enables us to realize high etching performances, where the etching rate of SiO_2, selectivities of SiO_2/resist, and SiO_2/Si were 340 nm/min, 6.8 and 31, respectively, in optimal condition. To clarify the plasma chemistry using solid material evaporation, CF_x ($x=1-3$) radical densities and F atom density were measured by infrared diode laser absorption spectroscopy and actinometric optical emission spectroscopy, and fluorocarbon films deposited on SiO_2 were analyzed by x-ray photoelectron spectroscopy. On the basis of these results, the etching mechanism was discussed. [DOI: 10.1116/1.1513632]

I. INTRODUCTION

Dry etching of silicon oxide (SiO_2) films is an essential process for fabricating deep contact holes in ultra-large-scale integrated (ULSI) circuits. This process has been developed by using high-density plasmas employing perfluorocompound (PFC) feed gases such as CF_4, CHF_3, C_2F_6, C_4F_8, and so on.[1–4] In this process, the high selectivity (SiO_2/Si and SiO_2/resist) and the vertical etching profile for high aspect ratio patterns are required. Especially, the high selectivity of SiO_2 over the resist mask together with Si as the underlayer is strongly required due to the decrease of the resist thickness.[5] As the critical dimension of sub-micron-size contact holes decreases, shorter wavelengths and a higher numerical aperture (NA) in the lithography process are required. The depth of focus diminishes more rapidly with increasing the NA. Hence, higher resolution requires shorter depth of focus and a thinner resist film process. Therefore, to overcome problems due to thin resist thickness, highly etching selectivity of SiO_2 over resist is strongly required. The etching reaction proceeds in competition with the polymer deposition on a wafer. Therefore, the polymer strongly affects the etching reaction. It is well known that CF_x ($x=1-3$) radicals in the plasma are important precursors of polymer deposition,[30] and thus significantly influence the etching characteristics.[6,7] Therefore, fluorocarbon chemistry involved in these radical reactions is indispensable to realize the high performance of highly selective etching of SiO_2 over Si and resist in ULSI circuits.

Furthermore, PFC feed gases cause a serious environmental problem, namely, global warming. The global warming potentials (GWPs) of PFC gases are estimated to be thousands of times as high as that of CO_2 gas because of their long lifetimes in the atmosphere. Therefore, the productive restriction on PFC gases has been intensively discussed and the use and production of PFC gases in industries must be prohibited.

Recently, in order to reduce PFC consumption in the plasma etching process, many researchers have carried out research of alternative gases and systems for the semiconductor manufacturing process. Etching processes employing low GWP gases have been studied as a reduction approach of the PFC. However, the use of alternative gases does not seem to be a final solution for preventing global warming because the influence of species dissociated from alternative gases on the environment has not been clarified yet.

In our previous study, an electron cyclotron resonance (ECR) plasma system using a solid material evaporation technique, where fluorocarbon species were generated from polytetrafluoroethylene (PTFE) by a CO_2 laser and injected into the plasma reactor, was developed and applied to SiO_2/Si selective etching, tungsten, and amorphous-Si etching processes.[8–12] The etching characteristics in ECR plasma employing the solid material evaporation technique were equivalent to those in a conventional ECR plasma employing

[a]Electronic mail: hori@nuee.nagoya-u.ac.jp

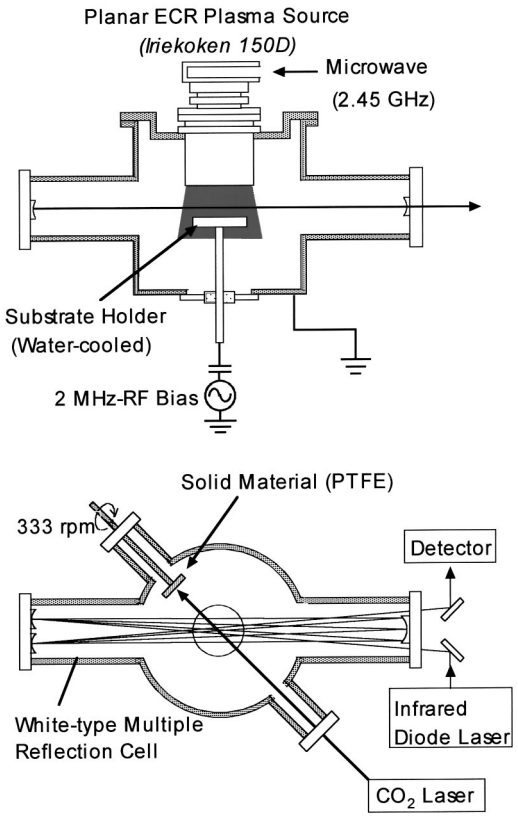

FIG. 1. Planar ECR plasma etching system equipped with the solid material evaporation system.

C_4F_8 gas. In this solid material evaporation technique, a solid material is used to replace PFC feed gases, and thus this system has many advantages. It enables us to reduce the capacity of the waste gas disposal apparatus because of the high exhaustion efficiency of reactive radicals coming from the plasma reactor compared with the stable PFC gases, and no risk for the leakage of fluorocarbon feed gases. Additionally, this system is very compact and safe because dangerous gas is not used and the gas cylinder is basically unnecessary.

In this study, SiO_2 contact hole etching was demonstrated by a planar ECR C_xF_y/Ar plasma employing a PTFE evaporation technique and etching characteristics such as etching rate, pattern profile, and selectivity of SiO_2 over resist were investigated by controlling the Ar dilution ratio and process pressure. CF_x $(x=1-3)$ radical densities and the F atom density were measured by infrared diode laser absorption spectroscopy (IRLAS) and actinometric optical emission spectroscopy (AOES), respectively. The fluorocarbon film deposited on SiO_2 was analyzed by x-ray photoelectron spectroscopy (XPS). On the basis of these measurements, the etching characteristics were discussed.

II. EXPERIMENT

Figure 1 shows a planar ECR plasma etching reactor equipped with a CO_2 laser evaporation system and IRLAS system. The planar ECR plasma source (IRIEKOKEN 150D), which employed permanent magnets to generate the magnetic field for ECR was used in the etching experiment. A 2.45 GHz microwave was introduced into the top of the reactor. An ECR region of 875 G was created approximately 1 cm below the quartz window.

In the solid material evaporation system, a cw CO_2 laser (10.6 μm), was used for evaporation of the PTFE targets. The cw CO_2 laser was very compact ($W70\times H97\times L425$ mm; SYNRAD, INC.) and its beam was irradiated on the surface of the PTFE target in the reaction chamber through the ZnSe window. The laser beam diameter was 3 mm. The radical flow rate was successfully controlled by CO_2 laser power.[8] The PTFE target was 5 mm in thickness. The molecular weight of PTFE is 107 g/mol and the melting point is 327 °C. The PTFE target was rotated at 333 rpm.

IRLAS is a very powerful diagnostic technique for *in situ* measurement of CF_x $(x=1-3)$ radicals in the plasma without disturbing the plasma.[13–17] A white-type multiple reflection cell, 200 cm in length, was installed in the process chamber to increase the absorption length of the infrared laser beam used for the radical density measurements. The laser beam passed 12 times for the measurement of CF_2 radical density at 2 cm above the substrate plate through the ECR plasma using the white-type multiple reflection cell and 40 times for those of CF and CF_3 radical densities. Absorption signals were detected by an infrared detector (MCT). The absorption lines used in this study were $R_1(7.5)$ and $R_2(7.5)$ lines for CF radicals,[18] ${}^{Q}R_4(26)$ line for CF_2 radicals,[19] and ${}^{R}R_{18}(18)$ line for CF_3 radicals.[20] The calculation procedures for the radical densities are described in Ref. 13. In these calculation procedures, the rotational temperature was assumed to be 350 K following a study by Haverlag *et al.*[21]

In the AOES measurements, a compact AOES-plasma monitor (PZ-M2; Opto Research Corporation) was used. The measured emission lines of F and Ar were a $[3s(^2P_2)-3p(^2P_2)]$ transition at 703.7 nm and a $[4s'(1/2)^0-4p'(1/2)]$ transition at 750.4 nm, respectively. The behavior of the F atom density ($\propto[I_{F*}/I_{Ar*}]\cdot N_{Ar}$) was examined by the AOES measurement.

X-ray photoelectron spectroscopy analysis enabled us to investigate the chemical structure of the fluorocarbon films. In the XPS system, the Mg $K\alpha$ line was used as an x-ray source.

III. RESULTS AND DISCUSSION

SiO_2 contact hole etching was performed using the ECR C_xF_y plasma employing the PTFE evaporation technique. A high etching rate (SiO_2) of 580 nm/min was obtained at a process pressure of 0.7 Pa. However, taper-etched profiles were observed because of excess deposition on the sidewalls of the contact holes. In order to improve the taper-etched profiles, Ar dilution effects were investigated at a process pressure of 0.7 Pa. Figure 2(a) shows the etching rate and selectivity (SiO_2/resist) as a function of Ar concentration ratio. The Ar concentration ratio means the partial pressure ratio ($Ar/[Ar+C_xF_y]$) in a fixed pumping speed. The etching rate of SiO_2 decreased slowly with increasing Ar concen-

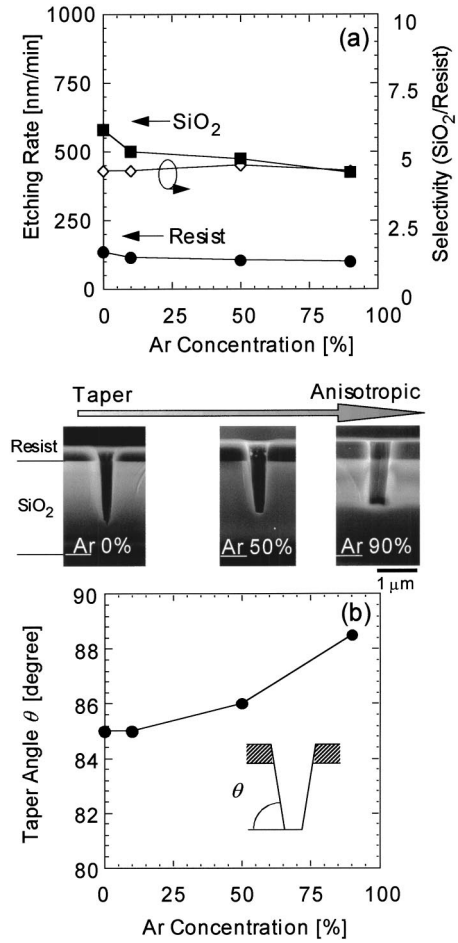

FIG. 2. Etching rate and selectivity (SiO_2/resist) as a function of the Ar concentration ratio and (b) taper angle as a function of the Ar concentration ratio at a microwave power of 400 W, process pressure of 0.7 Pa, bias voltage of −300 V, and pumping speed of 202 l/s.

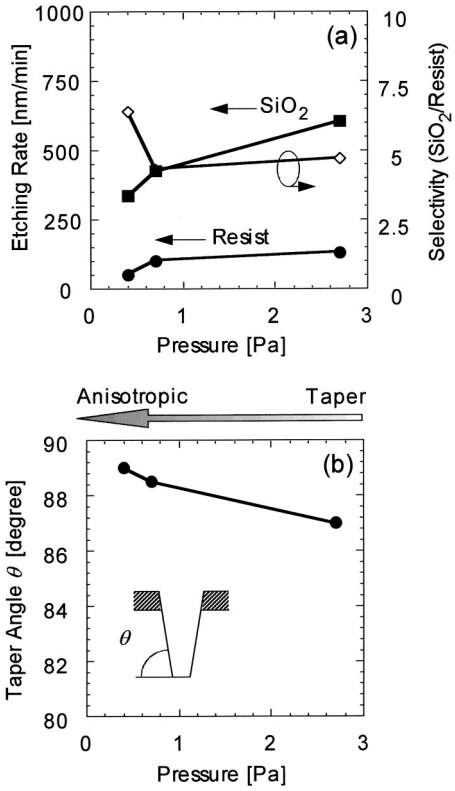

FIG. 3. Etching rate and selectivity (SiO_2/resist) as a function of the process pressure and (b) taper angle as a function of the process pressure at a microwave power of 400 W, Ar concentration ratio of 90%, and bias voltage of −300 V.

tration ratio and the etching rate of the SiO_2 was 430 nm/min at an Ar concentration ratio of 90%. The etching rate of the resist also decreased slowly with increasing Ar concentration and the etching rate of the resist was 100 nm/min at an Ar concentration ratio of 90%. As a result, the selectivity (SiO_2/resist) was almost constant (~4.3) against the Ar concentration ratio. Figure 2(b) shows the taper angle as a function of Ar concentration ratio. The taper-etched profile was improved with increasing Ar concentration ratio and the taper angle was 88.5°. From these results, the etched profile was successfully controlled by Ar dilution ratio in ECR Ar plasma with injection of species evaporated from PTFE.

It is well known that the vertical acceleration of ion species strongly depends on the process pressure. The dependence of the etching characteristics on the process pressure was also investigated at an Ar concentration ratio of 90%. The process pressure was varied from 0.4 to 2.7 Pa. Figure 3(a) shows the etching rate and selectivity (SiO_2/resist) as a function of the process pressure. The process pressure was controlled by changing the pumping speed in a fixed partial pressure ratio ($Ar/[Ar+C_xF_y]$). The etching rates of SiO_2 and the resist were 340 and 50 nm/min, respectively, at a process pressure of 0.4 Pa. The selectivity (SiO_2/resist) was 6.8 at a process pressure of 0.4 Pa. The etching rates of SiO_2 and the resist increased with increasing the process pressure, resulting in 610 and 130 nm/min, respectively, at a process pressure of 2.7 Pa. As a result, the selectivity (SiO_2/resist) decreased with increasing the process pressure and was 4.7 at a process pressure of 2.7 Pa. Figure 3(b) shows the taper angle as a function of the process pressure. The taper angle was 89° at a process pressure of 0.4 Pa. The taper angle decreased with increasing the process pressure and was 87° at a process pressure of 2.7 Pa. From these results, it has been found that the taper-etched profile is improved by increasing the Ar dilution ratio and decreasing the low process pressure.

It is considered that the taper angle is related to the fluorocarbon film deposition on the sidewall of the contact hole. The deposition rate (DR) of the fluorocarbon film on the SiO_2 blanket cut wafer was investigated. These experiments for evaluating the DR were performed without rf bias. Figure 4(a) shows the DR as a function of Ar concentration ratio. At an Ar concentration ratio of 0%, the DR was 80 nm/min. The DR decreased linearly with increasing Ar concentration ratio, resulting in 40 nm/min at an Ar concentration ratio of 90%. Figure 4(b) shows the DR as a function of the process pressure. At a process pressure of 0.4 Pa, the DR was 20 nm/min. The DR was increased with increasing the process pressure and was saturated. The DR reached 70 nm/min at a process

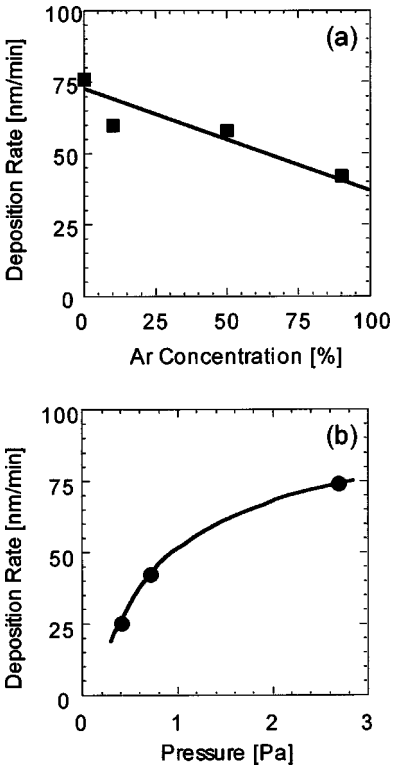

FIG. 4. (a) Deposition rate (DR) of the fluorocarbon films on the SiO_2 substrate as a function of the Ar concentration ratio at a microwave power of 400 W, process pressure of 0.7 Pa, bias voltage of −300 V, and pumping speed of 202 l/s. (b) DR as a function of the process pressure at a microwave power of 400 W, Ar concentration ratio of 90%, and a bias voltage of −300 V.

pressure of 2.7 Pa. Figure 5 shows the taper angle as a function of the DR obtained from the results shown in Figs. 2(b), 3(b), 4(a), and 4(b). The taper angle decreased linearly with increasing the DR. It exhibits that the taper angle depends on the DR of the fluorocarbon film. In the case of the lower DR, a highly anisotropic profile has been obtained.

Furthermore, the composition of the films was analyzed by using XPS. The F/C ratio of the films on the SiO_2 substrate was calculated from F 1*s* and C 1*s* intensities. Figure 6(a) shows the F/C ratio as a function of Ar concentration ratio. The F/C ratio was 0.90 at an Ar concentration ratio of

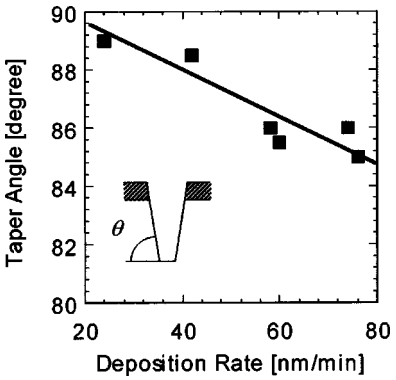

FIG. 5. Plot of the taper angle as a function of the DR.

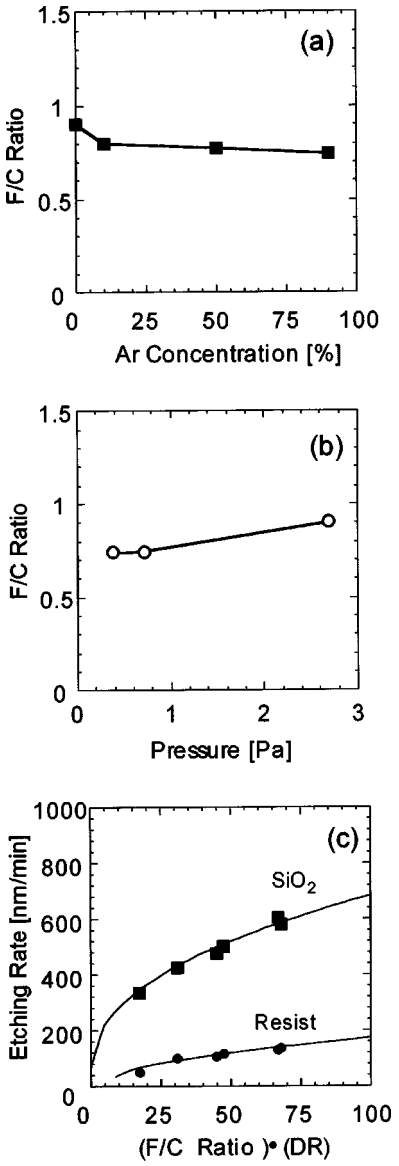

FIG. 6. (a) F/C ratio calculated from F 1*s* and C 1*s* intensities as a function of the Ar concentration ratio at a microwave power of 400 W, process pressure of 0.7 Pa, bias voltage of −300 V, and pumping speed of 202 l/s. (b) F/C ratio as a function of the process pressure at a microwave power of 400 W, Ar concentration ratio of 90%, and bias voltage of −300 V. (c) Plot of SiO_2 and resist etching rate as a function of the (F/C ratio)(DR).

0%. The F/C ratio decreased slowly with increasing the Ar concentration ratio and the F/C ratio was 0.75 at an Ar concentration ratio of 90%. Figure 6(b) shows the F/C ratio as a function of the process pressure. The F/C ratio increased with increasing the process pressure and was 0.91 at a process pressure of 2.7 Pa. The behaviors of the F/C ratio were similar to those of the etching rate of the SiO_2. Tatsumi *et al.* reported that the etching rate of SiO_2 was determined by the total number of the F atoms contained in the reaction layer.[22] Therefore, the relation between the etching rate on SiO_2 and the (F/C ratio) (DR) of the fluorocarbon films formed on the SiO_2 substrate was investigated. Figure 6(c) shows the etching rates of SiO_2 and the resist as a function of the (F/C ratio) (DR). The etching rates of SiO_2 and the resist in-

creased with increasing the (F/C ratio) (DR). It suggests that the etching rates of SiO_2 and the resist are closely related with the (F/C ratio) (DR) of the fluorocarbon film. In a (F/C ratio) (DR) of 0, SiO_2 is considered to be etched by only ion species. The etching rate of SiO_2 in a (F/C ratio) (DR) of 0 was estimated from the etching yield of CF_x^+ ions reported by Mayer, Barker, and Writman.[23] The etching rate by only ion species at the present condition (electron temperature: ~4 eV, electron density: $\sim 4.2\times10^{10}$ cm^{-3}) was estimated to be ~70 nm/min. This result indicates that the deposition of a F-rich thin layer enhances the etching rates of SiO_2 and the resist films with the bombardment of high-energy ions, where the bias voltage is −300 V.

Absolute densities of CF_x ($x=1-3$) radicals were measured by IRLAS to understand the behavior of these radicals. Figure 7(a) shows the CF_x ($x=1-3$) radical densities as a function of Ar dilution ratio. At an Ar concentration ratio of 0%, where the taper-etched profile was observed due to the excess deposition on the sidewall of contact holes, CF, CF_2, and CF_3 radical densities were 2.6×10^{12}, 1.4×10^{13}, and 2.5×10^{12} cm^{-3}, respectively. It is reported that the CF_2 radical is one of the precursors of the fluorocarbon polymer.[24–27,30] In this condition, where the CF_2 radical was the dominant species, excess deposition on the sidewall of the contact hole occurred. CF and CF_3 radical densities were independent of the Ar concentration ratio and were of the order on 10^{12} cm^{-3}. On the other hand, the CF_2 radical density was decreased with increasing the Ar concentration ratio and was 9×10^{11} cm^{-3} at an Ar concentration ratio of 90%. Figure 7(b) shows the F atom density measured by AOES as a function of the Ar concentration ratio. The F atom density decreased with increasing Ar concentration ratio. The decrease of the CF_2 radical and F atom densities with increasing the Ar concentration ratio seems to be due to the reduction of the C_xF_y molecular species.

In order to discuss what precursor contributes to the formation of the fluorocarbon films, the DRs, which were estimated from the CF_x ($x=1-3$) radical densities by the IRLAS measurement were compared with the experimental data of the DRs, as shown in Fig. 4(a). The DRs were estimated by the general expression

$$\mathrm{DR}=\frac{2s}{2-s}\Gamma\frac{M}{\rho}, \tag{1}$$

where s is the sticking probability and ρ is film density that was assumed to be 2.20 g/cm^{-3} (PTFE), which includes errors because the density of the deposited film will be somewhat different. The Γ is radical flux obtained by the general expression

$$\Gamma=\frac{1}{4}n\sqrt{\frac{8kT}{\pi M}}, \tag{2}$$

where n is the CF_x radical density, k is the Boltzmann constant, M is the mass of CF_x radicals, and T is the temperature of the CF_x radicals, which was assumed to be 350 K.

The sticking probability is a very important parameter to discuss the mechanism of deposition of films. However, they

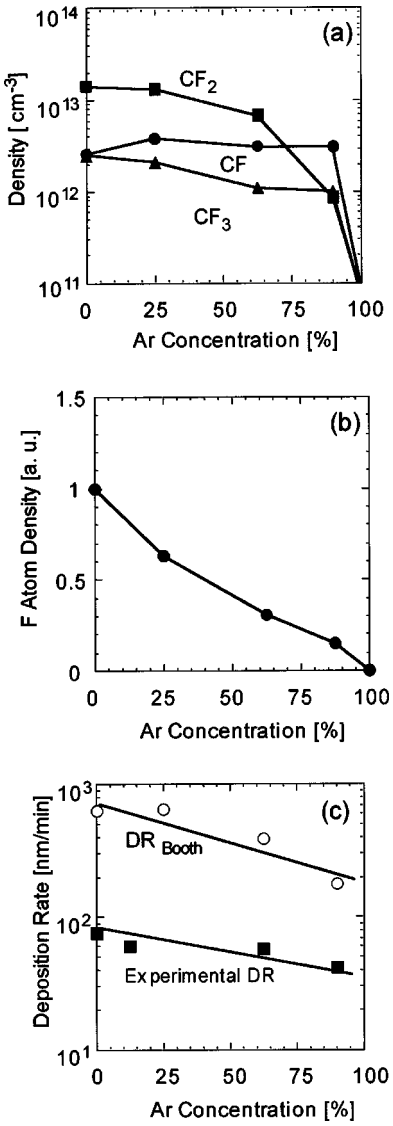

FIG. 7. (a) CF_x ($x=1-3$) radical densities and (b) F atom density as a function of the Ar concentration ratio at a microwave power of 400 W, process pressure of 0.7 Pa, bias voltage of −300 V, and a pumping speed of 202 l/s. (c) Experimental data of DR and DRs estimated from the CF_x radical densities as a function of Ar concentration at a microwave power of 400 W, process pressure of 0.7 Pa, and pumping speed of 202 l/s.

have not been sufficiently investigated. Several sticking probabilities of the CF_x ($x=1-3$) radicals were investigated.[28,29] Booth *et al.* investigated the sticking probabilities of the CF and CF_2 radicals in capacitively coupled plasma employing CF_4 gas. The sticking probabilities (steady state) of the CF and CF_2 radicals were estimated to be 2.4×10^{-1} and 1.5×10^{-1}, respectively, at a pressure of 27 Pa, a rf power of 0.1 kW, and substrate temperature of 20 °C.[28] Miyata, Hori, and Goto investigated the sticking probabilities of CF_x ($x=1-3$) radicals under low ion flux conditions in ECR C_4F_8 plasma. The sticking probabilities of the CF, CF_2, and CF_3 radicals were estimated to be 5×10^{-4}, 6×10^{-5}, and 2×10^{-3}, respectively, by a simulation study.[29]

Several researchers investigated the influence of ion spe-

cies on the sticking probabilities Takahashi *et al.* reported that the CF_2 radicals significantly contributed to the growth of fluorocarbon film with the assistance of plasma exposures using the radical injection technique.[30] Furthermore, Inayoshi *et al.* clarified the mechanism of fluorocarbon film formation through CF_2 radicals where ion species created the surface active sites that were dangling bonds, and CF_2 radicals were readily polymerized through these active sites, resulting in forming fluorocarbon films.[31] Oehrlein *et al.* reported that the deposition rate of fluorocarbon film on the substrate increased with increasing the ion bombardment in ECR CHF_3 plasma.[32] Considering these influences of ion species, the DR obtained in this study was analyzed using the sticking probabilities (steady state) of the CF and CF_2 radicals reported by Booth *et al.*

Figure 7(c) shows the experimental data of DR and DR_{Booth} estimated from the CF_x radical densities as a function of Ar concentration ratio. Here, the sticking probabilities reported by Booth *et al.* were used. The DR_{Booth} (open-circle symbol) indicated the same behavior as the experimental DR. However, it was higher than the experimental DR (filled-square symbol) by one order of magnitude. Considering the effect of etching through F atoms as shown in Fig. 7(b), the estimated deposition rate should increase because the F atom density decreases with increasing the Ar concentration ratio. Therefore, the etching effect of the F atom on the fluorocarbon film is negligibly small. This difference between the experimental DR and DR_{Booth} seems to be caused by the substrate temperature. The substrate temperature in this study was 100 °C, which was five times higher than that in Booth's study.

In a previous study, it was reported that higher species such as C_2F_4 and C_xF_y contributed to the formation of PTFE-like film under the condition of relatively low plasma density ($\leqslant 1.8\times 10^{10}$ cm^{-3}) and the CF_x radicals contributed to the formation of fluorocarbon films under the condition of high plasma density ($\geqslant 1.8\times 10^{10}$ cm^{-3}).[33] Teii *et al.* reported that higher species drastically decreased with increasing the microwave power and the Ar dilution ratio using an electron attachment QMS.[34,35] Therefore, the density of the higher species will be quite low at the present condition. Considering these results, it is considered that the CF_x radicals dominantly contribute to the formation of fluorocarbon films in this study.

Figure 8 shows the scanning electron microscopy (SEM) images of the 0.6 μm contact hole and 0.08 μm trench etched in the optimum condition (Ar concentration ratio of 90%, process pressure of 0.4 Pa). It has been found that high etching selectivity (SiO_2/resist=6.8, SiO_2/Si=31) and the anisotropic profile are obtained at a low process pressure (0.4 Pa) by using the ECR C_xF_y/Ar plasma system employing the PTFE evaporation technique. Therefore, the technique will be very useful for SiO_2 over the Si selective etching process in next-generation ULSI circuits, keeping harmony with the environment, particularly for preventing global warming.

From the viewpoint of preventing global warming, the effluent component from the etching chamber and the abatement system are also very important. Several researchers reported abatement systems employing plasma. Fiala *et al.* and Tonnis *et al.* investigated plasma abatement with an inductively coupled plasma after turbomolecular pumps.[36,37] Tonnis *et al.* examined the performance of an inductively coupled plasma abatement device for treatment of exhaust from a commercial, magnetically enhanced reactive ion etcher. Using either O_2 or H_2O vapor as abatement additives, PFC destruction and removal efficiencies of greater than 95% were successfully obtained for most process conditions tested. One way to eliminate by-products is to use the above plasma abatement system. The combination of our new gas source with the abatement system will be very powerful in completing an environmentally benign system.

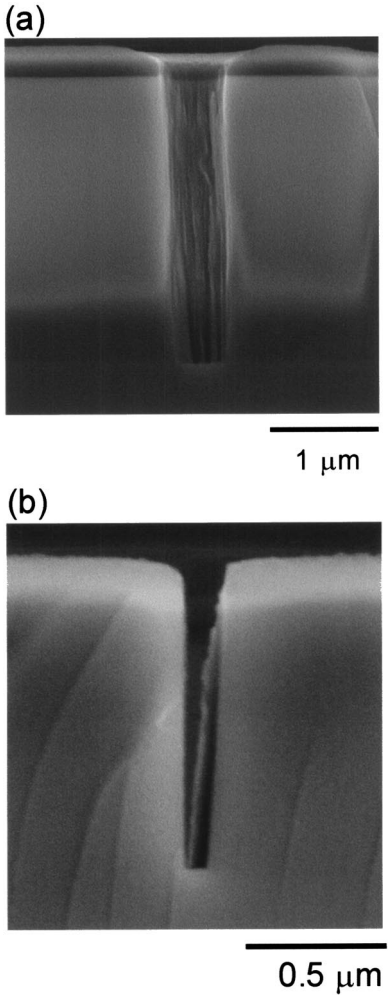

FIG. 8. SEM images of (a) 0.6 μm contact hole and (b) 0.08 μm trench etched in the optimum condition (Ar concentration ratio of 90%; process pressure of 0.4 Pa).

IV. CONCLUSIONS

A contact hole etching process has been performed by using an ECR C_xF_y/Ar plasma system employing the PTFE evaporation technique. This system employs no PFC feed gas which causes the global warming problem, and furthermore, it is very safe and compact. The etched profile was

successfully controlled by varing the Ar dilution ratio and process pressure. The vertical profile was achieved under high Ar dilution (90%) and low pressure (0.4 Pa) condition. In the optimal condition, a 0.6 μm contact hole and a 0.08 μm trench were etched vertically and the etching rate of SiO_2, the selectivities of SiO_2 /resist, and SiO_2/Si were 340 nm/min, 6.8, and 31, respectively. The behaviors of the CF_x ($x=1-3$) radical densities and F atom density were clarified by IRLAS and AOES, and the fluorocarbon film deposited on SiO_2 was analyzed by XPS. From these results, it has been found that the etching rate of SiO_2 corresponds to the product of the F/C ratio of the film composition and deposition rate, and then the CF_x radicals contribute dominantly to the etching rate and selectivity of SiO_2 over the resist. This technique will be applicable to the SiO_2 fine contact hole etching process, keeping harmony with the environment, particularly for preventing global warming.

ACKNOWLEDGMENTS

This work is partially supported by NEDO. The authors would like to thank the Mitsui Dupont Fluorochemical Company for supplying the PTFE targets in this work. The authors would like to thank T. Ohkura of the Opto Research Corporation for allowing them to use the AOES plasma monitor.

[1]O. Joubert, G. S. Oehrlein, and Y. Zhang, J. Vac. Sci. Technol. A **12**, 658 (1994).
[2]O. Joubert, G. S. Oehrlein, and M. Surendra, J. Vac. Sci. Technol. A **12**, 665 (1994).
[3]S. Arai, K. Tsujimoto, and S. Tachi, Jpn. J. Appl. Phys., Part 1 **31**, 2011 (1992).
[4]R. d'Agostino, P. Capezzuto, G. Bruno, and F. Cramarossa, Pure Appl. Chem. **57**, 1287 (1985).
[5]Y. S. Kim, P. T. C. Wei, G. R. Tynan, R. Charatan, and D. Hemker, Jpn. J. Appl. Phys., Part 1 **37**, 327 (1998).
[6]K. Takahashi, M. Hori, S. Kishimoto, and T. Goto, Jpn. J. Appl. Phys., Part 1 **33**, 4181 (1994).
[7]L. M. Ephrath, J. Electrochem. Soc. **126**, 1419 (1979).
[8]K. Fujita, M. Ito, M. Hori, and T. Goto, J. Vac. Sci. Technol. B **17**, 957 (1999).
[9]K. Fujita, M. Ito, M. Hori, and T. Goto, J. Vac. Sci. Technol. A **17**, 3260 (1999).
[10]K. Fujita, S. Kobayashi, M. Ito, M. Hori, and T. Goto, Mater. Sci. Semicond. Process. **2**, 219 (1999).
[11]K. Fujita, S. Kobayashi, M. Ito, M. Hori, and T. Goto, Jpn. J. Appl. Phys., Part 1 **40**, 832 (2001).
[12]K. Fujita, S. Kobayashi, M. Ito, M. Hori, and T. Goto, J. Vac. Technol. (submitted).
[13]M. Magane, N. Itabashi, N. Nishiwaki, T. Goto, C. Yamada, and E. Hirota, Jpn. J. Appl. Phys., Part 2 **29**, L829 (1990).
[14]K. Maruyama, K. Ohkouchi, Y. Ohtsu, and T. Goto, Jpn. J. Appl. Phys., Part 1 **33**, 4298 (1994).
[15]K. Takahashi, M. Hori, and T. Goto, Jpn. J. Appl. Phys., Part 1 **33**, 4745 (1994).
[16]K. Miyata, K. Takahashi, S. Kishimoto, M. Hori, and T. Goto, Jpn. J. Appl. Phys., Part 2 **34**, L444 (1995).
[17]K. Miyata, M. Hori, and T. Goto, J. Vac. Sci. Technol. A **14**, 2343 (1996).
[18]K. Kawaguchi, C. Yamada, Y. Hamada, and E. Hirota, J. Mol. Spectrosc. **102**, 193 (1983).
[19]P. B. Davies, W. Lewis-Bevan, and D. K. Russell, J. Chem. Phys. **75**, 5602 (1981).
[20]C. Yamada and E. Hirota, J. Chem. Phys. **78**, 1703 (1983).
[21]M. Harverlag, E. Stoffels, W. W. Stoffels, G. M. W. Kroesen, and F. J. de Hoog, J. Vac. Sci. Technol. A **14**, 380 (1996).
[22]T. Tatsumi, M. Matsui, M. Okigawa, and M. Sekine, J. Vac. Sci. Technol. B **18**, 1897 (2000).
[23]T. M. Mayer, R. A. Barker, and L. J. Whitman, J. Vac. Sci. Technol. **18**, 349 (1981).
[24]R. d'Agostino, F. Cramarossa, V. Colaprico, and R. d'Ettole, J. Appl. Phys. **54**, 1284 (1983).
[25]S. Samukawa and S. Furuoya, Jpn. J. Appl. Phys., Part 2 **32**, L1289 (1993).
[26]J. A. O'Neill and J. Singh, J. Appl. Phys. **77**, 497 (1995).
[27]T. Goto and M. Hori, Jpn. J. Appl. Phys., Part 1 **35**, 6521 (1996).
[28]J. P. Booth, G. Cunge, P. Chabert, and N. Sadeghi, J. Appl. Phys. **85**, 3097 (1999).
[29]K. Miyata, M. Hori, and T. Goto, Jpn. J. Appl. Phys., Part 1 **36**, 5340 (1997).
[30]K. Takahashi, M. Hori, M. Inayoshi, and T. Goto, Jpn. J. Appl. Phys., Part 1 **35**, 3635 (1996).
[31]M. Inayoshi, M. Ito, M. Hori, T. Goto, and M. Hiramatsu, J. Vac. Sci. Technol. A **16**, 233 (1998).
[32]G. S. Oehrlein, Y. Zhang, D. Vender, and M. Haverlag, J. Vac. Sci. Technol. A **12**, 323 (1994).
[33]K. Fujita, M. Ito, M. Hori, and T. Goto, J. Appl. Phys. (submitted).
[34]K. Teii, M. Hori, T. Goto, and N. Ishii, J. Appl. Phys. **87**, 7185 (2000).
[35]K. Teii, M. Hori, T. Goto, and N. Ishii, J. Vac. Sci. Technol. A **18**, 1 (2000).
[36]A. Fiala, M. Kiehlbauch, S. Mahnovski, and D. B. Graves, J. Appl. Phys. **86**, 152 (1999).
[37]E. J. Tonnis, D. B. Graves, V. H. Vartanian, L. Beu, T. Lii, and R. Jewett, J. Vac. Sci. Technol. A **18**, 393 (2000).